



## EISCAT\_3D

Time, Frequency and Synchronisation Subsystem Report

EISLAB, LTU

Gustav Stenberg

December 9, 2008



# Contents

<b>1</b>	<b>Overview</b>	<b>5</b>
1.1	About this document . . . . .	5
1.2	Introduction . . . . .	5
1.2.1	In-phase clock distribution . . . . .	6
<b>2</b>	<b>Simulation</b>	<b>7</b>
2.1	Steering & Amplitude . . . . .	7
2.2	Beamwidth . . . . .	7
2.3	Simulation Conclusions . . . . .	7
<b>3</b>	<b>Cable-based calibration</b>	<b>12</b>
3.1	Simulation Results . . . . .	12
3.1.1	Notes . . . . .	12
<b>4</b>	<b>GNSS-based calibration</b>	<b>14</b>
4.1	Timing system concept . . . . .	14
4.2	GNSS simplified receiver . . . . .	14
4.3	Test Setup for concept evaluation . . . . .	16
4.4	Results . . . . .	16
<b>5</b>	<b>Conclusions</b>	<b>21</b>

## List of Figures

2.1	Steering accuracy plot for 36-taps optimized filter set. 1000 runs at each jitter setting on the 12-by-4 test array. . . . .	8
2.2	Amplitude accuracy plot for 36-taps optimized filter set. 1000 runs, array 12-by-4 at jitter 160 ps, amplitude jitter $\approx 0.187$ dB. The red bar marks the ideal amplitude that would be achieved if no errors were introduced. . . . .	9
2.3	Beam-forming amplitude jitter as a function of time jitter. With a limit of -0.2 dB, $\sim 161$ ps of timing jitter is acceptable. . . . .	10
2.4	Beamwidth test run for the 12-by-4 test array with 160 ps timing jitter included. The $0.06^\circ$ maximum beamwidth demand is met only for elevations above $\sim 20^\circ$ . There are barely visible peaks that shows the limited but existent effect of jitter on the beamwidth. . . . .	11
3.1	Diagram of the EISCAT_3D LAAR racks containing the cable calibration system. Each LNA is connected to every other LNA in the array via the <i>CALIBRATION LINK</i> to allow calibration of the different units to each other. . . . .	13
4.1	Diagram of the EISCAT_3D LAAR receiver front-end and GNSS timing unit. . . .	15
4.2	Measured and expected phase difference between test- and reference antennas. Dashed lines indicates the expected phase differences calculated from the antenna position difference and current satellite geometry, and the solid lines indicates the actually measured phase differences. Integer ambiguity is not resolved in this plot and the data has been unwrapped to make the plot more perspicuous. No averaging has been applied to the data. . . . .	17
4.3	Baseline error between test- and reference antennas. The dashed lines indicates that a 5 min averaging filter has been applied. . . . .	18
4.4	Time difference between test- and reference antennas. The dashed lines indicates that a 5 min averaging filter has been applied. . . . .	19
4.5	Histogram of the time difference between test- and reference antennas using 50 bins. The standard deviation of the data is 50.11 ps. No averaging has been applied to this data. . . . .	20

# 1 Overview

## 1.1 About this document

The requirement on the timing system of a digital phased-array antenna is very stringent since both the pointing and the shape of the beam is decided by the combined signals from all the antenna elements through time delay of the signal from the individual antenna elements in the array. Thus, one of the main research areas for the EISCAT\_3D project has been time and frequency synchronization throughout the array.

This document serves as a short report on the necessary demands, the work done on synchronization, which includes two different approaches, and finally the results and conclusions on the time and frequency synchronization.

## 1.2 Introduction

The general demand on the EISCAT\_3D project is that it should be ten times better in every aspect than the existing EISCAT system. That gives the demand of  $0.6^\circ$  pointing accuracy on the antenna array. By calculation, this yields the accuracy of the phase-shift in each antenna element to be  $\sim 6^\circ$ . That relates to a 50 ps accuracy in the sampling time of each element throughout the entire antenna array. In reality, this limit is somewhat relaxed, and as shown by the simulations in Chapter 2, a timing accuracy with a standard deviation of  $\sim 160$  ps will be sufficient [1]. However, this timing limit is composed of all timing errors; timing distribution system, jitter in ADCs, antenna phase center movement due to weather, etc. Thus, it is reasonable that the target accuracy of the *timing distribution system* is 50 ps.

The inherent properties of antenna array gives that the actual pointing accuracy varies with the angle of the beam. This is because the pointing error and the width of the beam are inversely proportional to the effective antenna aperture. When the beam is moved away from the normal of the array, i.e. towards the horizon, this area will be smaller and thus the error and beamwidth will be larger. With this in mind, all calculations and test have been made at worst-case to give robust results.

There are two different approaches to solving the timing distribution system for EISCAT\_3D. The first system is a cable-based system that continuously evaluates the delay between different parts of the timing system, thereby keeping track of any shifts in delay through the system. The second one is based on Global Navigation Satellite Systems (GNSS), which tracks the difference in phase of the signals from satellites to the timing units placed in the center of each sub-array [2].

There are benefits and drawbacks of both systems: The cable-based system is less prone to disturbances but needs a lot of cables in the array and can only run when the radar is off. The GNSS-based system could be sensitive to disturbances since it is based on radio signals, but if disturbances are significant to the GNSS signal, chances are that the radar itself also is unusable. The GNSS system has a lot less hardware requirements, i.e. almost no cables, and thus could be a lot cheaper in a large array.

### 1.2.1 In-phase clock distribution

To be able to achieve a 50 ps accuracy in the timing within the array, it is not enough to distribute only a clock to all elements, the phase of the clock also has to be distributed. The main problem with such short times as we are looking at is that one no longer can look at the speed of light as infinite, i.e. we have to take delays into account. Actually, 50 ps is only about 1.5 cm in length! See Eq. 1.1. With this distance the assumption is made that the signals actually travels with the speed of light, which probably won't be the case. In an ordinary coaxial cable, the propagation speed is usually around 60-80% of  $c$ , making the critical distance even shorter.

$$\begin{aligned} l &= v \cdot t \\ &= 2.99\text{E}^8 \cdot 50\text{E}^{-12} = 1.499 \text{ cm} \end{aligned} \tag{1.1}$$

The easiest way of achieving phase coherence within the array would be to use cable lengths that are multiples of the distance that is one wavelength of the distributed clock. Doing so, all of the elements in the array will always have the same phase. However, there are some major drawbacks of this approach. First, the accuracy will be highly dependent on the fabrication and mounting. Second, even differences in the cable lengths due to heat differences over the array, e.g. parts of the array is in sunlight and the rest in shade, produce significant errors. Finally, such a system would have no way of self-calibration, since the phase would solely depend on the length of the interconnecting wires.

## 2 Simulation

The first step of the development of the timing and frequency synchronization system was to evaluate the actual demands on the system itself. These requirements stem from the defined properties of the EISCAT\_3D system, such as beamwidth and pointing accuracy. To evaluate the actual impact of the pointing accuracy that the timing of the array actually has, large amounts of calculations are needed. In this aspect it was decided that a model of the whole antenna system should be created in Matlab.

In the following sections are the results of these simulations that reveals the necessary level of accuracy required by the EISCAT\_3D system.

### 2.1 Steering & Amplitude

One of the main design criteria is the steering accuracy of the beam. This aspect is mainly affected by the ability to correctly delay the signal from each antenna element, i.e., the element-to-element time jitter of the system. Sample-to-sample jitter in the ADC is expected to be less than one ps. The jitter simulations are time consuming, especially when statistical accuracy is desired. In our case, each jitter simulation consists of 1000 runs with Gaussian distributed time jitter. As can be seen in Figure 2.1, the steering accuracy easily meets the  $\pm 0.03^\circ$  criteria for timing jitters up to 250 ps. Instead, the beam-forming loss criteria of  $\leq 0.2$  dB sets the maximum allowable time jitter to  $\sim 160$  ps, see Figures 2.2 & 2.3.

### 2.2 Beamwidth

The beamwidth simulations were done with  $\sigma = 160$  ps Gaussian distributed time jitter which proves good enough in respect to the timing jitter for the timing distribution system of EISCAT\_3D as long as the jitter is independent, see Figure 2.4. The beam shape does not change considerably due to the evenly distributed time jitter, but is more prone to distortion if linear errors are introduced over the array. This stresses the point that the timing of the S&H circuits over the whole array not only must be accurate, but any errors must be close to independent.

As seen in Figure 2.4, the  $0.06^\circ$  maximum beamwidth demand is met only for elevations above  $\sim 20^\circ$ . However, this may be remedied by using a different layout of the array to increase the aperture for low elevations or placing the array on a hillside to achieve the same effect.

### 2.3 Simulation Conclusions

As noted above, the necessary accuracy on the timing system is a maximum standard deviation of 160 ps. It is reasonable to attribute about a third of this variation to the timing distribution system itself, thus a target accuracy of 50 ps is valid.

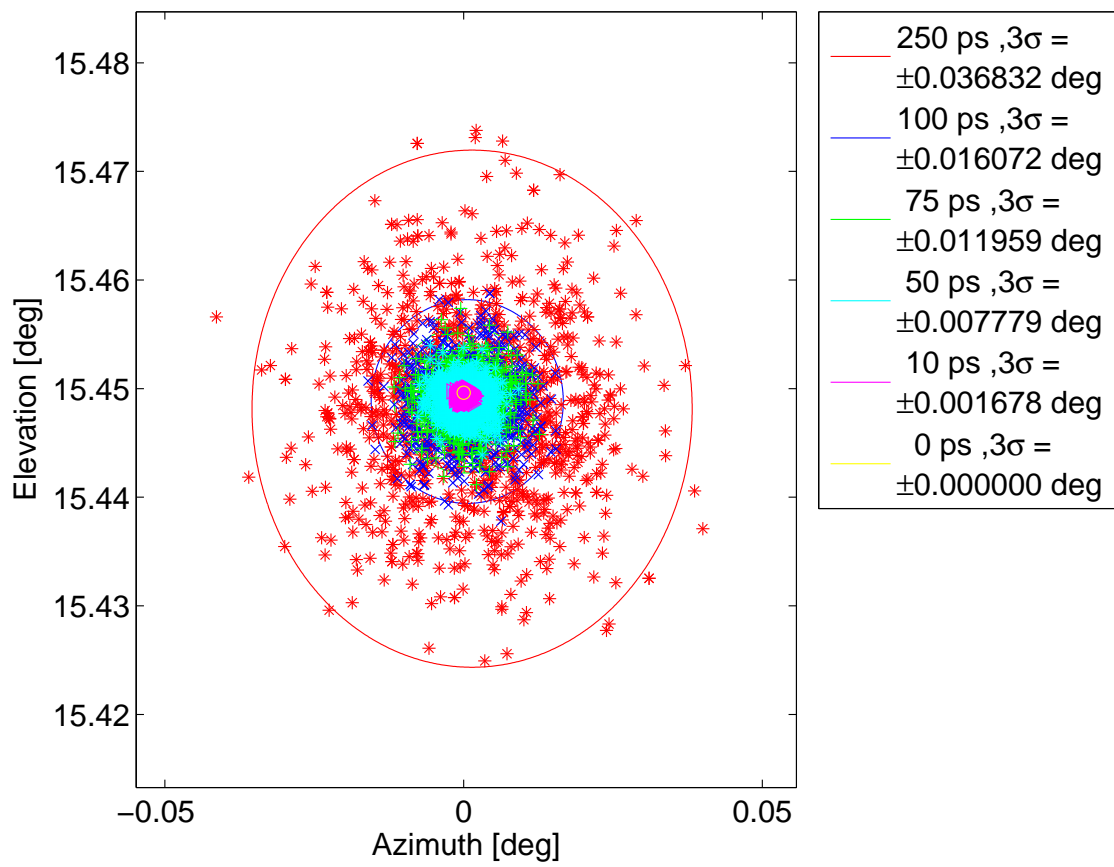


Figure 2.1: Steering accuracy plot for 36-taps optimized filter set. 1000 runs at each jitter setting on the 12-by-4 test array.

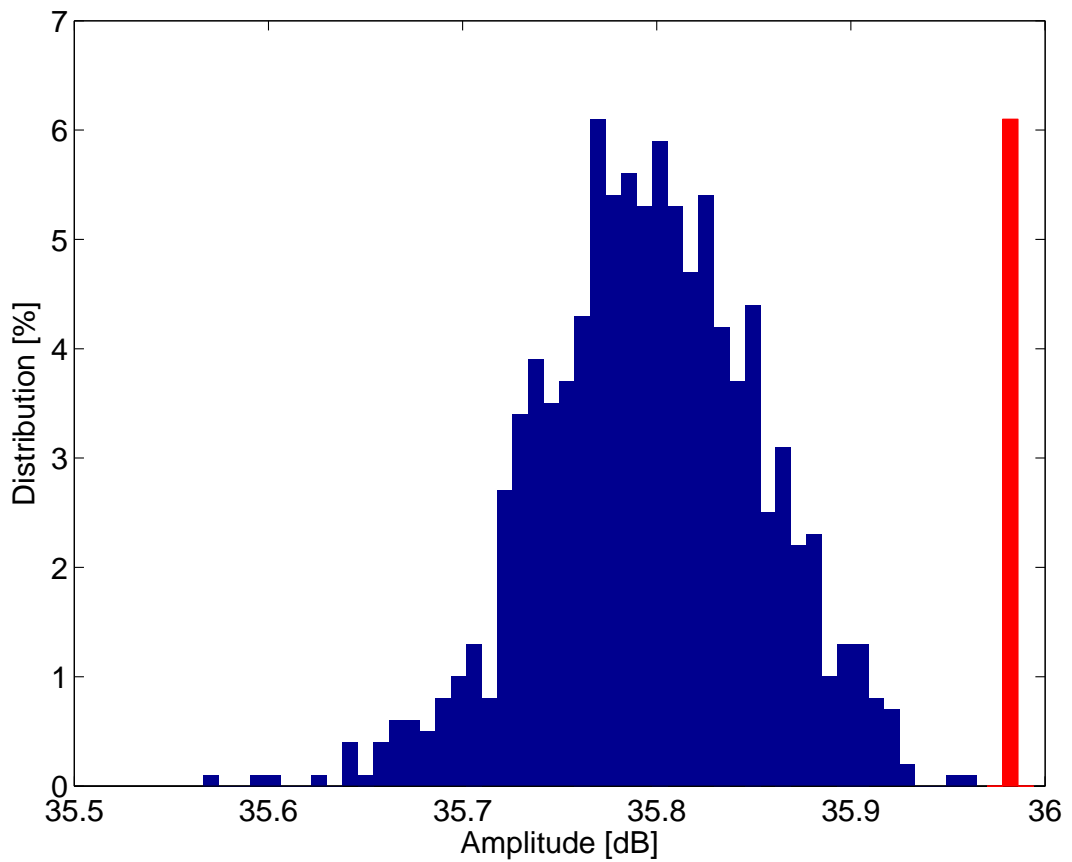


Figure 2.2: Amplitude accuracy plot for 36-taps optimized filter set. 1000 runs, array 12-by-4 at jitter 160 ps, amplitude jitter  $\approx 0.187$  dB. The red bar marks the ideal amplitude that would be achieved if no errors were introduced.

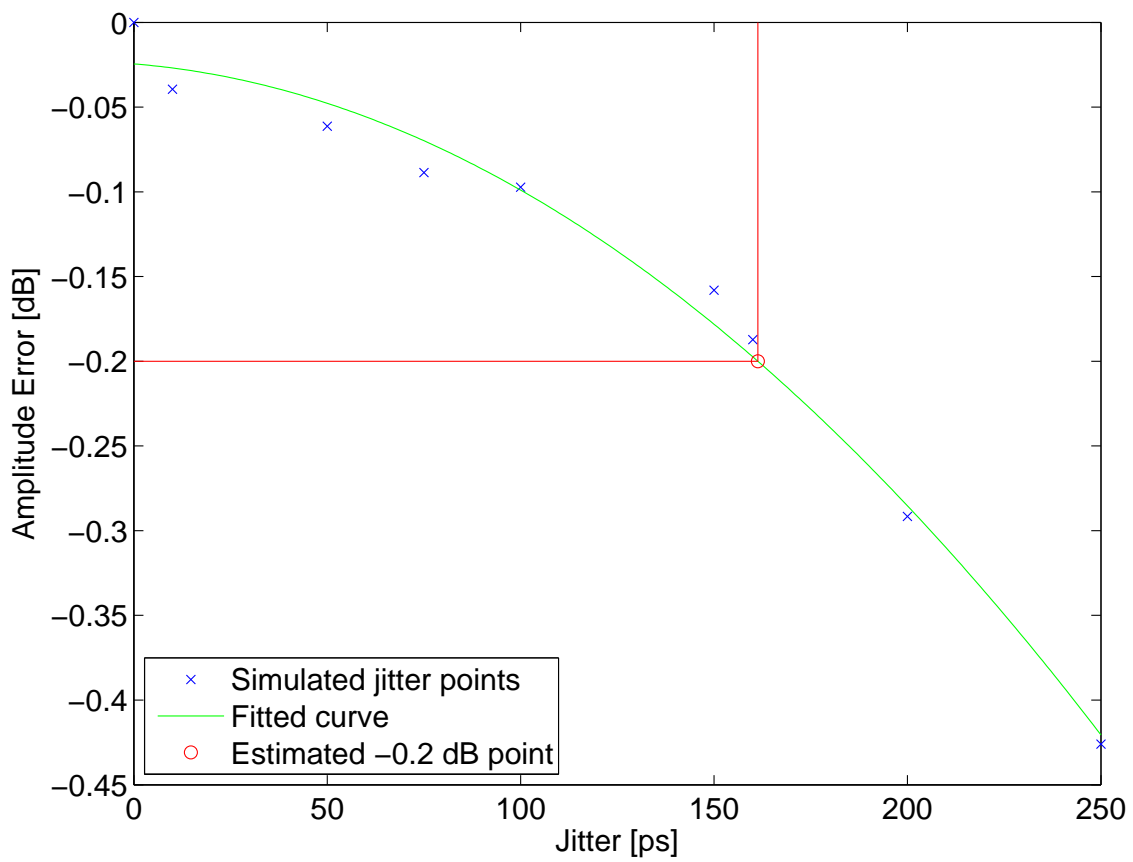


Figure 2.3: Beam-forming amplitude jitter as a function of time jitter. With a limit of -0.2 dB, ~161 ps of timing jitter is acceptable.

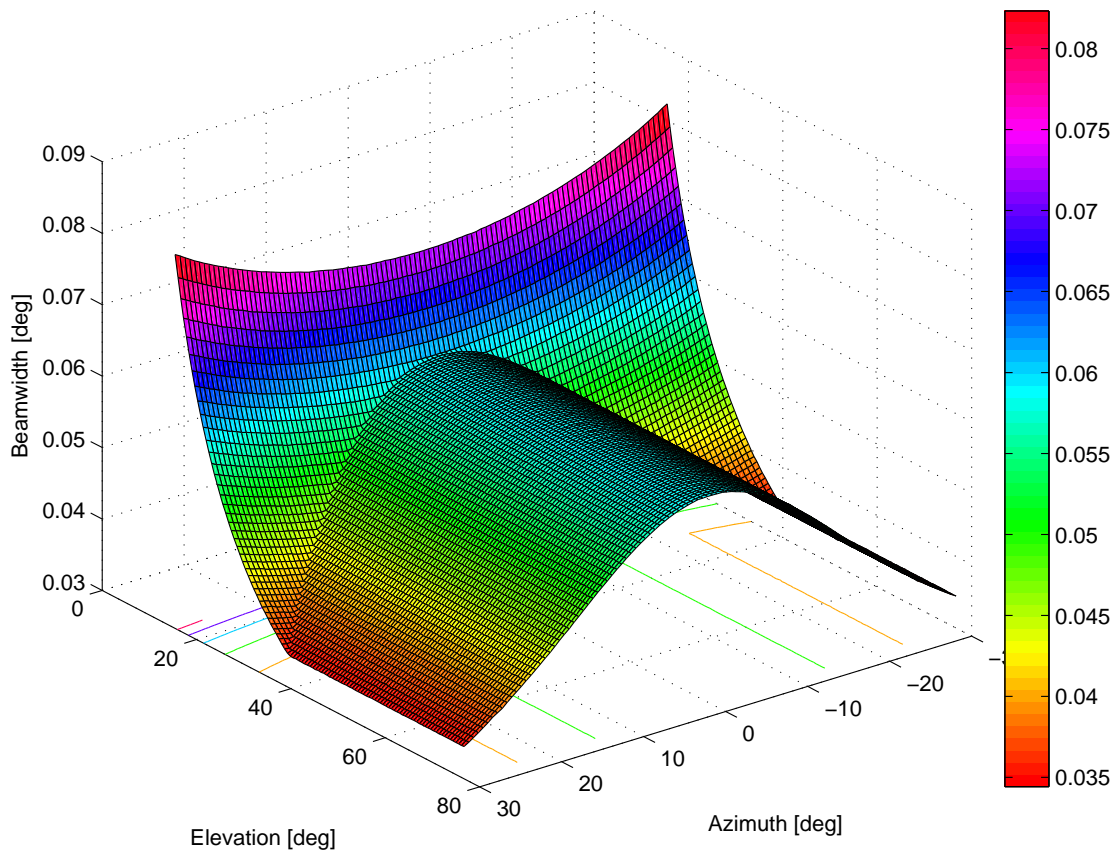


Figure 2.4: Beamwidth test run for the 12-by-4 test array with 160 ps timing jitter included. The  $0.06^\circ$  maximum beamwidth demand is met only for elevations above  $\sim 20^\circ$ . There are barely visible peaks that shows the limited but existent effect of jitter on the beamwidth.

## 3 Cable-based calibration

One way of achieving phase synchronization was first suggested by Grover[3]. The idea is to send a pulse down a line and let it reflect at the end point, measuring the average time between the outgoing and reflected pulses. By doing so, one actually measures the time of the reflection, regardless of where on the line you are positioned when doing the measurement. Thus, using only one line for the whole array, each antenna element measures the same time with great accuracy. By synchronizing another distributed clock with this measurement, one would achieve phase-synchronized clocks in the whole array.

This method would prove difficult to achieve in the EISCAT\_3D project, mainly because of difficulties in keeping the signal levels large enough through the array and to create a sensor with good enough accuracy to measure the time of each pulse. However, a version of the system has been developed where each LNA of the system is connected to every other LNA, see Figure 3.1. By injecting a sinusoid signal in the LNAs in different order and with different frequency, the actual relationship between the length of the cables used for the calibration can be decided. The direction of the injected signal can also be controlled, so that the length of signal path can be deduced not only between the LNAs, but also from each LNA to the phase center of the connected antenna and also through the normal signal chain to the ADC.

### 3.1 Simulation Results

The cable calibration system simulation is built up by connecting n-ports representing different parts of the system using the function `ConnectS.m` in Matlab.

Using capacitance matrices that should correspond to the coupler on the coupler/LNA pcb's and deviations of 0.02, which seems consistent with the variations seen between the manufactured coupler boards.

The coupler board switches are modeled by a 3 ohm On-resistance and 1.25 pF terminal capacitances, with deviations 0.1 common and 0.02 difference between switches. The resistors are set to  $R_2=40$ ,  $R_3=5$ ,  $R_4=220$ ,  $R_5=220$  (dev=0.02). This should give something in the order of 20 dB local signal injection attenuation.

If we set the antenna and front-end reflections to  $-(10..13)$  dB and  $-(15..18)$  dB (chosen randomly), respectively, we get delay and amplitude standard variations of 32 ps and 6.0%, which can probably still be considered "ok". Increasing LNA reflections to  $-(10..13)$  dB increases the error to 45 ps and 7.7 % respectively. Both these tests meet the required 50 ps target for the timing system.

#### 3.1.1 Notes

The current calculations of front-end doesn't attempt to make any corrections for "known" errors, e.g if we make production measurements on the coupler/LNA boards, nor does it compensate for the limited directivity of the coupler (which results in antenna impedance "measurements" being way off).

Most parts of the simulator back-end as well as several "blocks" was implemented by Jonas Lindström.

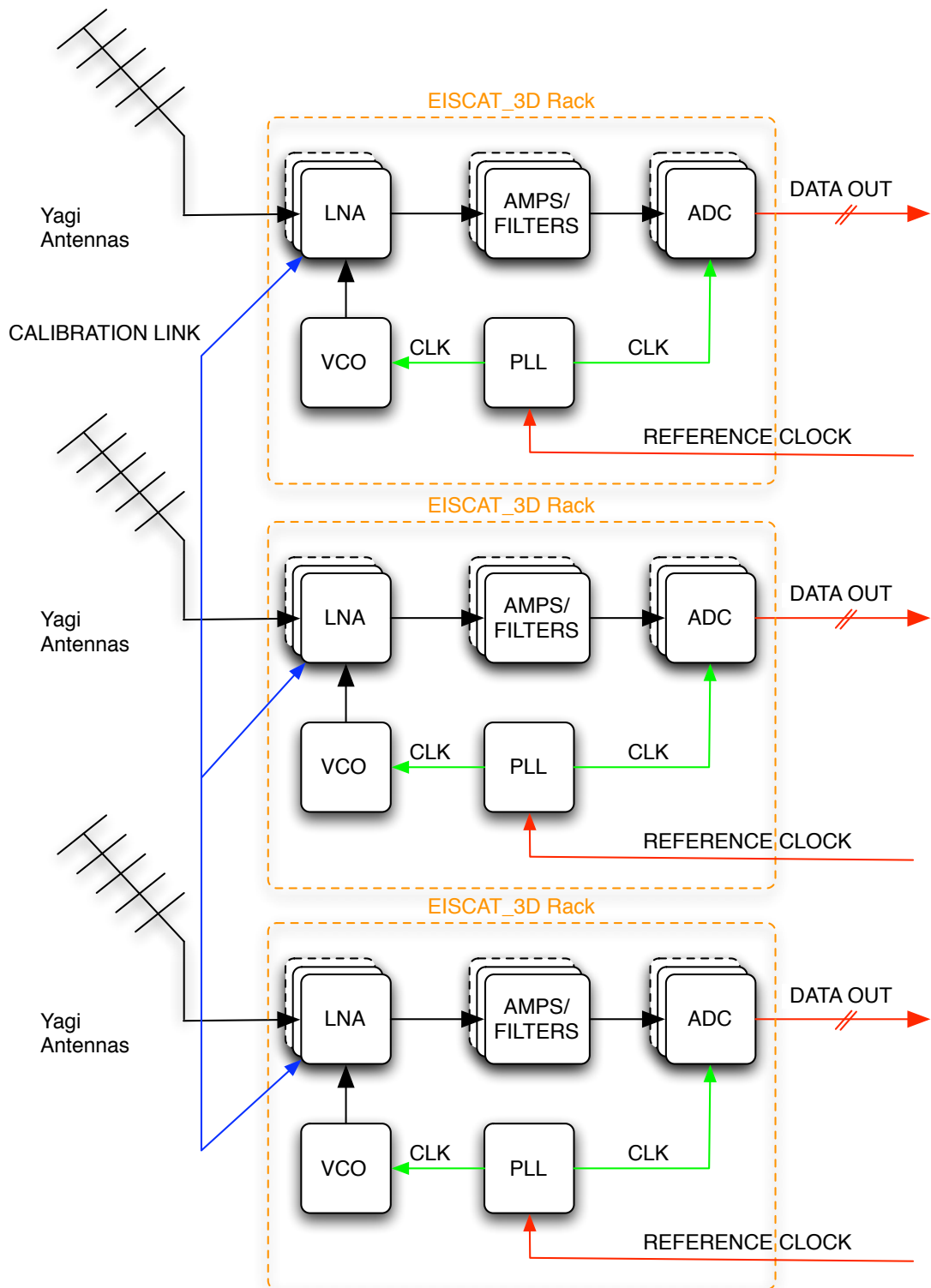


Figure 3.1: Diagram of the EISCAT\_3D LAAR racks containing the cable calibration system. Each LNA is connected to every other LNA in the array via the *CALIBRATION LINK* to allow calibration of the different units to each other.

## 4 GNSS-based calibration

In the system described here, low-end L1-only GNSS receivers are used in a highly application specific environment, to provide the picosecond accuracy timing. This is done by dividing the LAAR into small sub-arrays of e.g. 16 elements each. The maximum length of the cables distributing the clock is then reduced to 6 m which is short enough to be calibrated by length approximation only, assuming that the clock distributed to each sub-array is known. By inserting a Global Navigation Satellite System (GNSS) receiver at each of these sub-arrays, to provide a clock reference that is unaffected by changing conditions over the array, the antennas are now timed to the specified accuracy.

Other benefits of building a GNSS timing system include lower cost due to reduced amount of coaxial cable throughout the array, and that a continuous cable length calibration system that ensures the timing accuracy of the distributed clock system is no longer necessary.

The following sections will describe in detail the concept of designing an L1-only GNSS receiver based timing system which is highly application specific to meet the requirements of the EISCAT\_3D LAAR. The simplifications that are possible to make to the GNSS receivers are stated and then a test setup made as proof of concept of the timing system is described.

### 4.1 Timing system concept

Each of the sub-arrays will contain a Phase Locked Loop (PLL) in which the distributed frequency reference is reproduced and distributed to the local GNSS receiver, the radar ADCs, and a signal injection system located as close to the radar antenna elements as possible to calibrate the analog signal path of the system, as shown in Figure 4.1.

The main purpose of the PLL is to adjust the phase of the reference clock to be equal throughout the array. This is achieved by creating a closed loop feedback from the GNSS receiver to the PLL and adjusting the phase according to the phase differences in the received satellite signals in respect to a reference GNSS receiver. The reference receiver is a high-end receiver which is used in conjunction with application specific software to produce the information sent to each of the sub-array receivers that is necessary to calculate the phase difference of the local clock compared to the reference clock. The PLL can now be used to make the needed adjustments so that all local clocks have the same phase throughout the array.

The information sent from the reference GNSS receiver to each of the GNSS timing units is; which satellites to use, Doppler-shift, tracking chip, and expected phase and time. This information will allow the sub-array receivers to only be capable of tracking a low number of satellites, no more than six, and using the tracked phase differences to calculate the expected phase of the local PLL. Thus, full capability receivers are not needed, but instead an Field-Programmable Gate Array (FPGA) will be used with a GNSS RF-frontend to control the PLL.

### 4.2 GNSS simplified receiver

In general, an off-the-shelf GNSS L1-receiver is rated to produce a clock with an error of less than 50 ns, which is about 1000 times higher than the necessary 50 ps accuracy. However, specific conditions apply to this GNSS timing system that improves the accuracy and will relax the requirements on the receiver, such as:

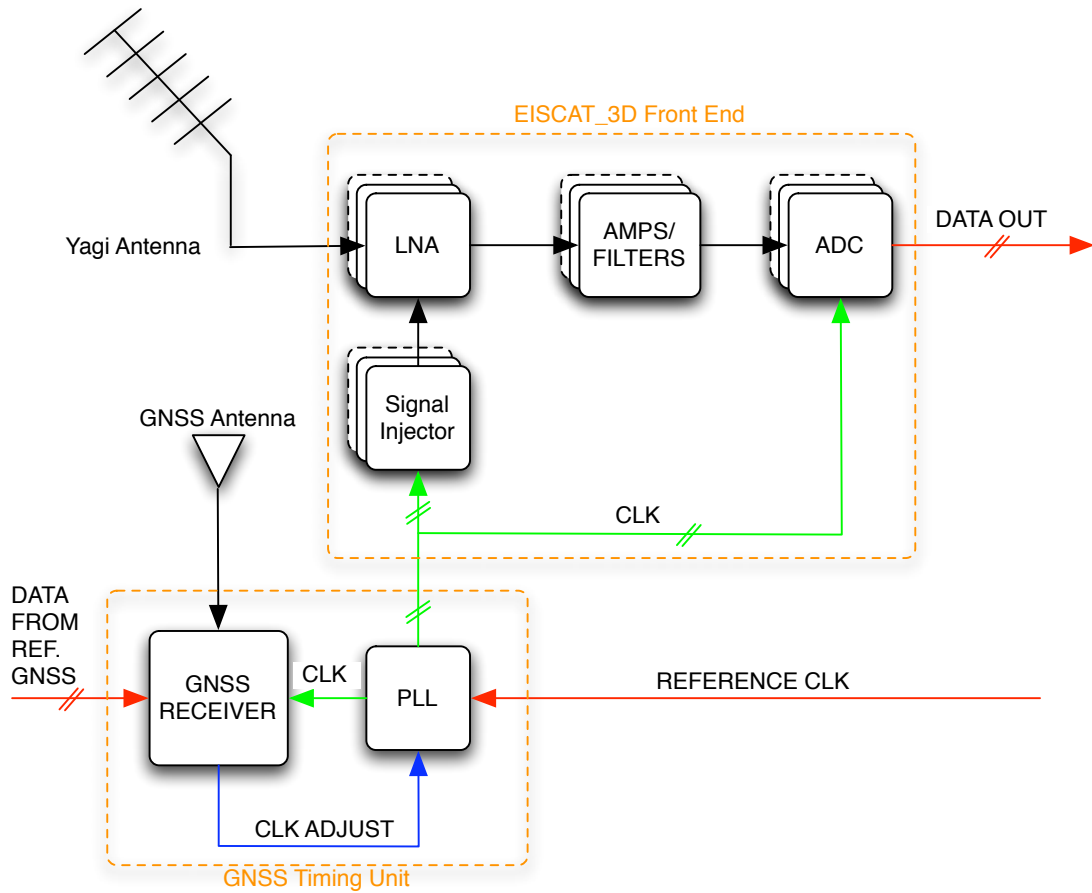


Figure 4.1: Diagram of the EISCAT\_3D LAAR receiver front-end and GNSS timing unit.

- A short base-line system, i.e. the maximum distance between two GNSS antennas is 300 m which infer all significant external errors, such as atmospheric, ionospheric, and ephemeris errors, in this application to be common over the array.
- A common high accuracy reference clock is available throughout the array to all receivers, which removes a significant part of the clock drift errors between the receivers.
- Externally based selection of which satellites are to be used for the position & time solution to exclude any timing errors arising from the use of different geometry matrices in the position & time calculations.
- All receivers are stationary and the time constant of the change of cable length in the reference clock distribution can be expected to be in the order of 30 min. This enables the use of a very long integration time, up to 30 min, of the timing solution which will reduce thermal noise significantly.
- Phase measurements from one satellite only is sufficient to calculate the timing error between the sub-arrays since the relative position of each receiver is known with good ac-

curacy. However, more satellites will increase accuracy and also reduce any positional error of the GNSS antenna.

- No integer ambiguity solution is necessary, since the relative position of the receivers is known with good accuracy and the absolute time difference between the receivers is insignificant, only the phase of the distributed clock is important.

These conditions all relax the requirements on each of the GNSS timing units to the point where each timing unit only need to be capable of tracking a low number of satellites, measuring the phase of each satellite and then calculate the timing and position error of it's own location relative to the reference antenna. With the use of a FPGA, the correlators and tracking can be built in hardware and the calculation part can be built in software with the use of existing processing cores that are available for many FPGAs, all within a single chip.

### 4.3 Test Setup for concept evaluation

Test measurements have been performed in an outdoor environment during windy winter conditions, clear weather at  $-10^{\circ}\text{C}$  and wind speeds up to 20 m/s in gusts, with two antennas (Novatel GPS-702-GG) placed randomly, but precisely surveyed, at approximately 5 m distance from each other placed on a rooftop to simulate the conditions in the EISCAT\_3D LAAR. Intermediate Frequency (IF) data from the antennas were collected during a one hour measurement with a NordNav Multi-FrontEnd receiver and then post-processed in a Matlab script to calculate time and position difference between the antennas. As clock reference a rubidium frequency standard (PRS10, Stanford Research Systems, Inc.) was used.

The software used for post-processing is in-house developed and includes all the necessary functions that a future FPGA-based GNSS timing unit would need, such as tracking, phase calculation and position & time estimation. The position & time estimator is based on the Least-Squares estimator to provide better accuracy when the equation system is overdetermined. The actual equation used is based on equation (7.14) in [4]. Since the integer ambiguity ( $N$ ) is known in this case, the equation will be reduced to

$$(\phi_{ar} + N_{ar})\lambda = \mathbf{G} \begin{bmatrix} \mathbf{x}_{ar} \\ b_{ar} \end{bmatrix} + \varepsilon_{\phi,ar} \quad (4.1)$$

where  $\phi_{ar}$  is the phase difference between the test- and reference antennas,  $N_{ar}$  is the integer ambiguity,  $\lambda$  is the wavelength of the carrier signal,  $\mathbf{G}$  is the geometry matrix,  $\mathbf{x}_{ar}$  is the position difference  $b_{ar}$  is the time difference, and  $\varepsilon_{\phi,ar}$  is the remaining errors. Subscripts  $a$  indicates test antenna and  $r$  the reference antenna.

This equation is solvable for the unknowns  $\mathbf{x}_{ar}$  and  $b_{ar}$  giving the Least-Square estimation of the position and time difference between the test antenna and the reference antenna.

When running the post-processing a time resolution of 0.5 s was chosen for each position & time solution. This resolution should as a minimum be achievable in a future hardware implementation of the system.

### 4.4 Results

After running the post-processing on the collected data, the expected and measured phase differences between the test- and reference antennas were plotted for each tracked satellite, see Figure 4.2. The expected and measured values are almost identical except for a bias that

differs from satellite to satellite. The bias is an indication of a timing difference between the two antennas, or rather the receivers connected to the antennas. The sign of the bias in this plot differs simply because the plot ignores the integer ambiguity for clarity.

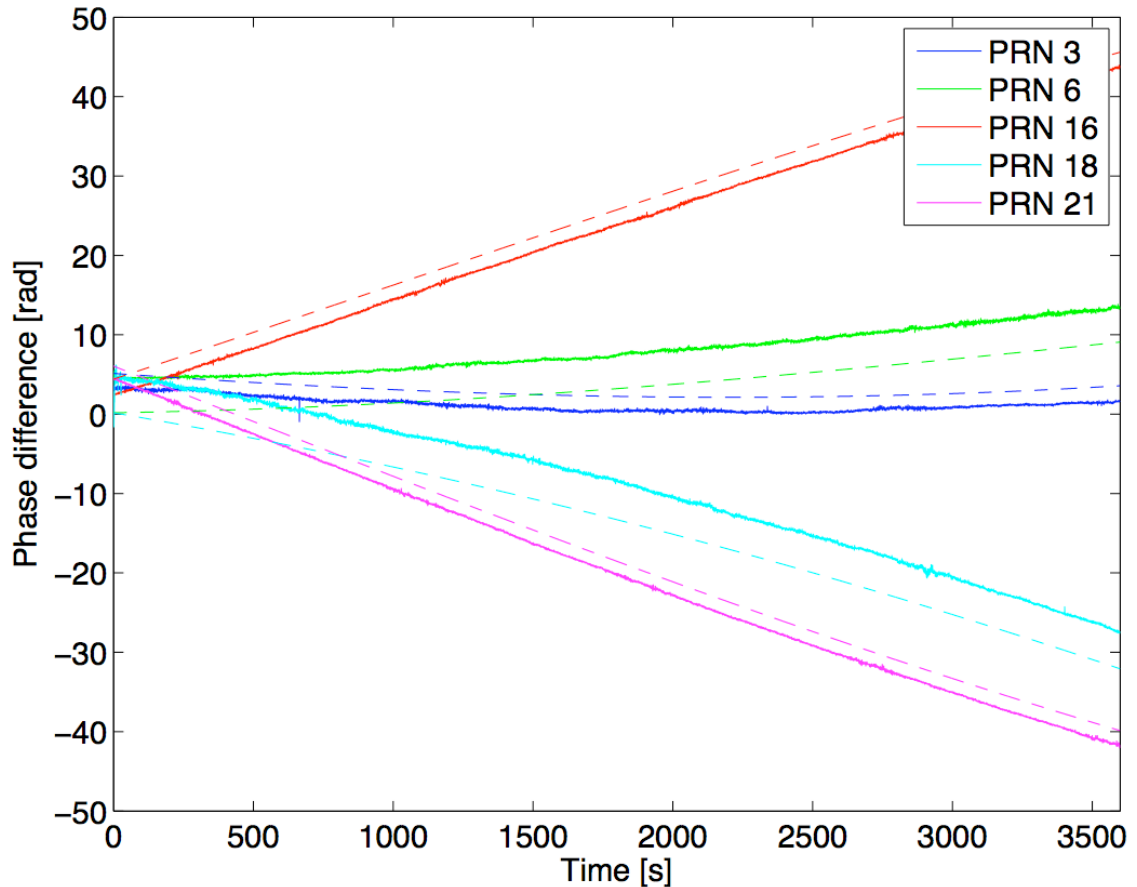


Figure 4.2: Measured and expected phase difference between test- and reference antennas. Dashed lines indicates the expected phase differences calculated from the antenna position difference and current satellite geometry, and the solid lines indicates the actually measured phase differences. Integer ambiguity is not resolved in this plot and the data has been unwrapped to make the plot more perspicuous. No averaging has been applied to the data.

After solving Equation 4.1 for all collected data points,  $d\mathbf{x}_{ar}$  was plotted to give an insight in the accuracy of the system, see Figure 4.3. The baseline error seen in the figure has a standard deviation of  $\sigma_x = 14.77$  mm,  $\sigma_y = 4.97$  mm, and  $\sigma_z = 13.93$  mm respectively in ECEF-coordinates.

An averaging filter of 5 min of data was also applied to the solution to achieve a less noisy measurement which is indicated in the figure with a dashed line. When using the filter, the standard deviation is reduced to  $\sigma_x = 4.50$  mm,  $\sigma_y = 1.88$  mm, and  $\sigma_z = 6.63$  mm respectively.

The  $b_{ar}$  values were also plotted, see Figure 4.4, with and without the 5 min averaging filter. It is obvious from the figure that a clock bias exists between the two receivers, which can be detected with this setup and calculated with relatively simple means, see Equation 4.1.

Without averaging, the standard deviation of the clock difference is  $\sigma = 50.11$  ps, which is

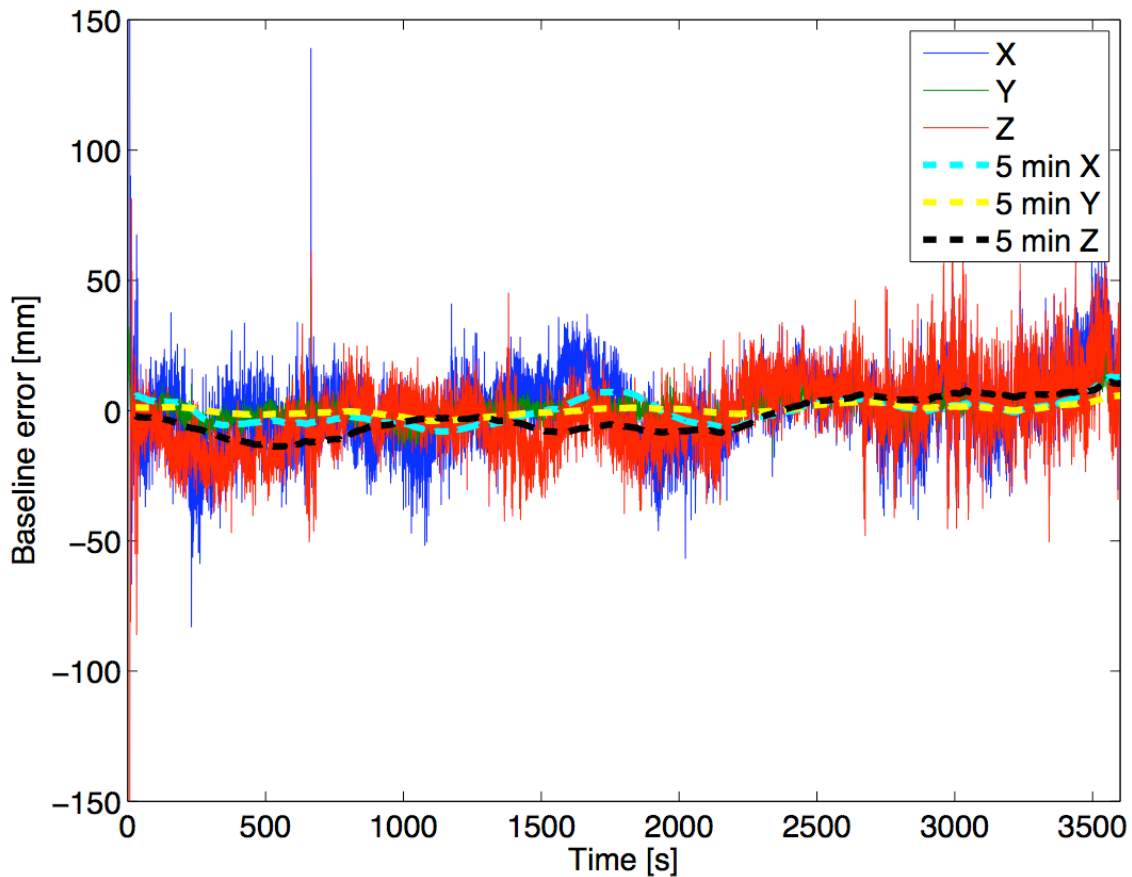


Figure 4.3: Baseline error between test- and reference antennas. The dashed lines indicates that a 5 min averaging filter has been applied.

within the usability range for the timing of the EISCAT\_3D LAAR. With the 5 min averaging filter applied, this is reduced to  $\sigma = 20.52$  ps. To ensure that the oscillations in Figure 4.4 are actually a normally distributed timing error, a histogram of the time difference is shown in Figure 4.5.

The use of a GNSS based picosecond accuracy timing system has been shown to be feasible to achieve using relatively simple calculations. The need for a timing error of less than 50 ps for the EISCAT\_3D LAAR has been met with margin using only 5 min of integration time, yielding a timing error of approximately 21 ps.

Due to the simplifications of the GNSS position & time calculations possible for the highly application specific conditions that apply for the EISCAT\_3D LAAR, a GNSS timing unit can be created in an FPGA to a relatively low cost compared to other timing distribution solutions.

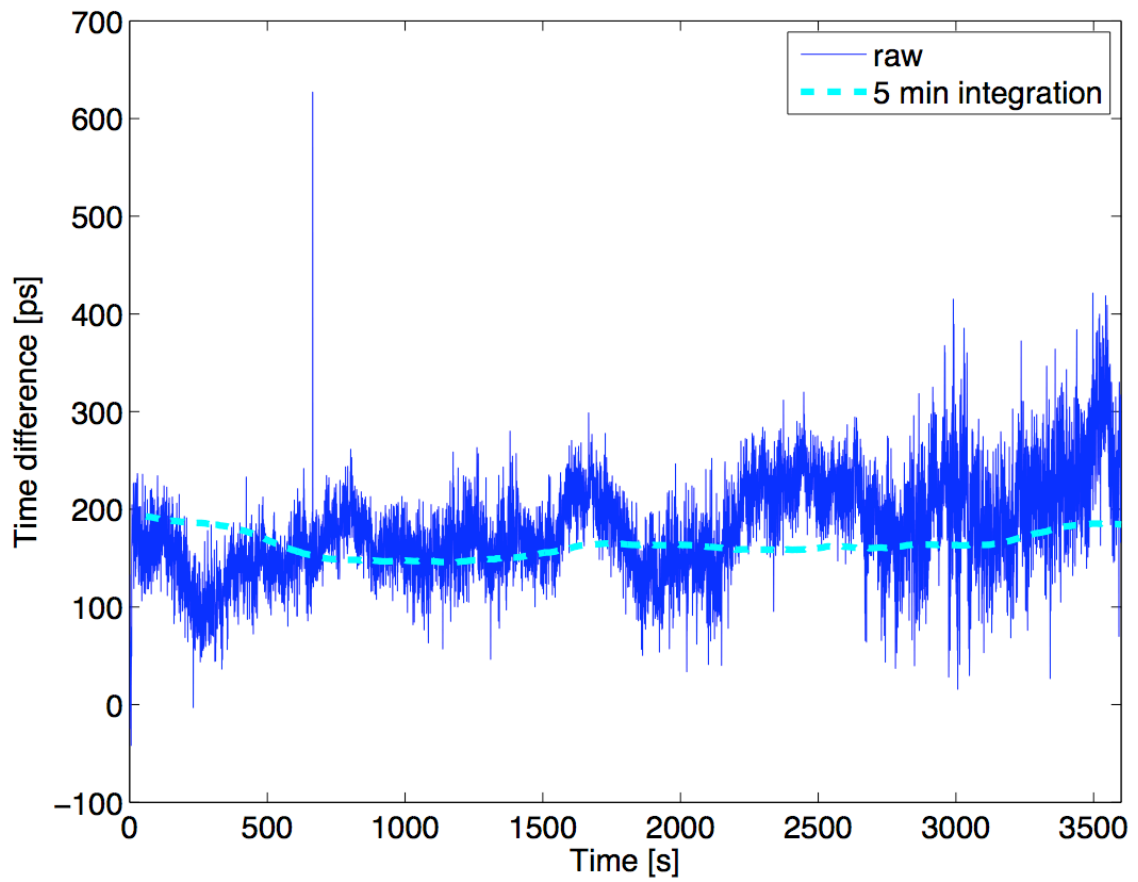


Figure 4.4: Time difference between test- and reference antennas. The dashed lines indicates that a 5 min averaging filter has been applied.

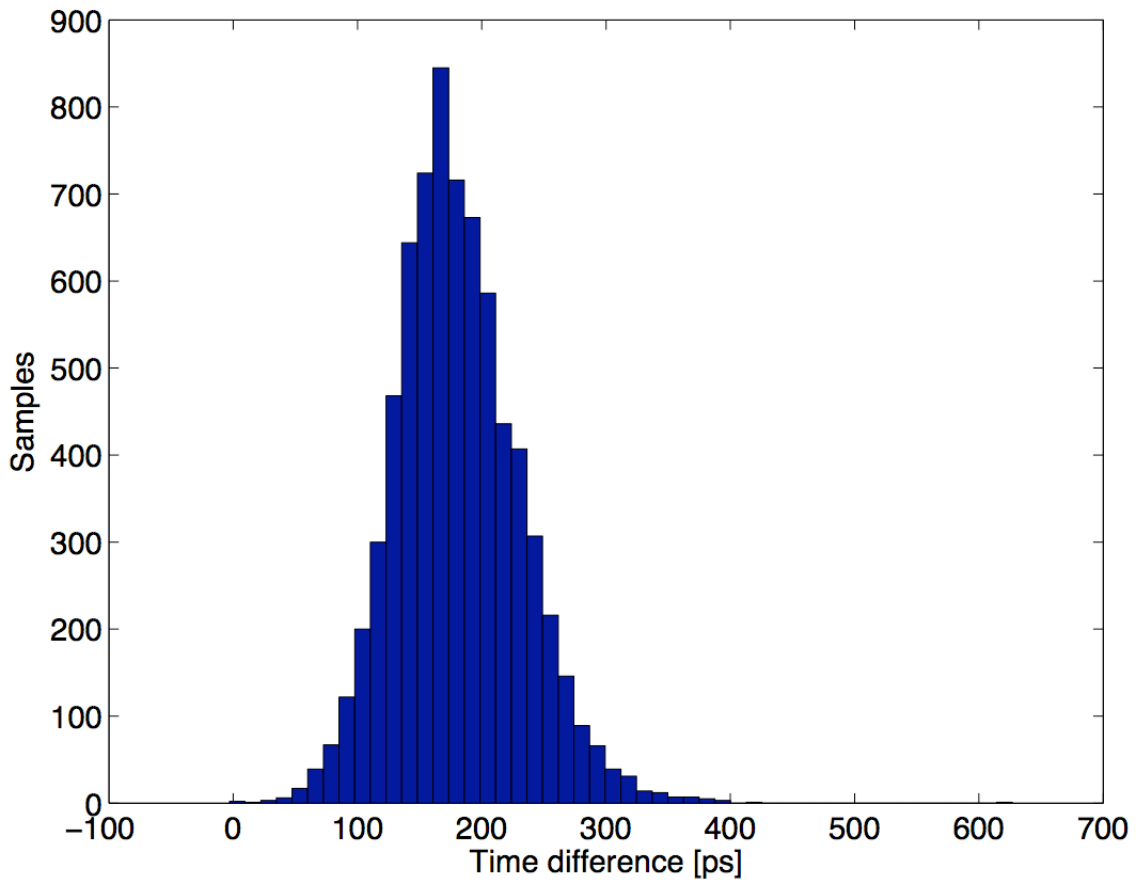


Figure 4.5: Histogram of the time difference between test- and reference antennas using 50 bins. The standard deviation of the data is 50.11 ps. No averaging has been applied to this data.

## 5 Conclusions

The exact requirements of the time and frequency synchronization system needed for the EISCAT\_3D project has been found by simulation. The most important requirement is the standard deviation of the sampling time of the ADC of each antenna throughout the array, which has to be better than 160 ps.

This requirement has been used as the target of the developed hardware, where 50 ps of the error have been allotted to the timing distribution system. Two different approaches has been evaluated for the timing distribution and are summarized below.

- The cable-based system has been evaluated in simulation and have an approximate standard deviation of 30-45 ps depending mostly on the reflection between front-end and antenna. The system has been built in hardware and is currently under evaluation in the test array in Kiruna. No real data yet.
- The GNSS-based system has been evaluated in hardware tests, but with a limited base-length and using post-processing. The results show that a standard deviation of 20 ps is readily achievable with simple calculations.

The main difference between the two systems is that the cable-based system uses more hardware than the GNSS-based system. On the other hand, the cable-based system is capable of not only calibrating the timing, but also the gain of each channel compared to the others.

At the current status of the project, all efforts are now put on the hardware tests of the cable-based calibration system installed in the test array.

## Bibliography

- [1] G. Stenberg, J. Borg, J. Johansson, and G. Wannberg, "Simulation of post-adc digital beamforming for large area radar receiver arrays," in *International RF and Microwave Conference*, 2006.
- [2] G. Stenberg, T. Lindgren, and J. Johansson, "A picosecond accuracy timing system based on l1-only gnss receivers for a large aperture array radar," in *ION GNSS 2008*. Institute of Navigation, 2008.
- [3] W. Grover, "A new method for clock distribution," *IEEE Trans. Circuits Syst. I, Fundam. Theory Appl. (USA)*, vol. 41, no. 2, pp. 149 – 60, Feb 1994.
- [4] P. Misra and P. Enge, *Global Positioning System, Signals, Measurements, and Performance*, 2nd ed. P.O. Box 692, Lincoln, Massachusetts 01773: Ganga-Jamuna Press, 2006.